Pion photoproduction in a dynamical coupled-channel model

F. Huang[*], M. Döring[†], H. Haberzettl[**,†], S. Krewald[†,‡] and K. Nakayama[*,†]

[*]*Department of Physics and Astronomy, University of Georgia, Athens, GA 30602, USA*
[†]*Institut für Kernphysik and Jülich Center for Hadron Physics, Forschungszentrum Jülich, 52425 Jülich, Germany*
[**]*Center for Nuclear Studies, Department of Physics, The George Washington University, Washington, DC 20052, USA*
[‡]*Institute for Advanced Simulations, Forschungszentrum Jülich, 52425 Jülich, Germany*

Abstract. Pion photoproduction reactions are investigated in a dynamical coupled-channel approach based on the Jülich πN model, which presently includes the hadronic πN and ηN stable channels as well as the $\pi\Delta$, σN and ρN effective channels. This model has been quite successful in the description of $\pi N \to \pi N$ scattering for center-of-mass energies up to 1.9 GeV. The full pion photoproduction amplitude is constructed to satisfy the generalized Ward-Takahashi identity and hence, it is fully gauge invariant. The calculated differential cross sections and photon spin asymmetries up to 1.65 GeV center-of-mass energy for the reactions $\gamma p \to \pi^+ n$, $\gamma p \to \pi^0 p$ and $\gamma n \to \pi^- p$ are in good agreement with the experimental data.

INTRODUCTION

In the past few years, intensive experimental efforts have taken place at major laboratories around the world to study the baryon spectra using the electromagnetic probes. On the theoretical side, since the baryon resonances are unstable and couple strongly to baryon-meson continuum states, coupled-channel models are needed to analyze the experimental data and to interpret the extracted resonance parameters. For our present study, we employ the well-known Jülich πN model [1–3] that is based on time-ordered perturbation theory. It is a coupled-channel meson-exchange model which includes the πN and ηN stable channels as well as the $\pi\Delta$, σN and ρN effective channels accounting for the resonant part of the $\pi\pi N$ channel. The interaction kernel corresponding to the t- and u-channel diagrams is constructed based on the chiral Lagrangians of Wess and Zumino [4], supplemented by additional terms for the coupling of Δ, ω, η, a_0 and σ [2, 3]. For the s-channel diagrams, apart from the bare nucleon dressed by the coupling to the πN continuum state to reproduce the physical nucleon, the interaction kernel includes eight genuine bare resonances, namely $S_{11}(1535)$, $S_{11}(1650)$, $S_{31}(1620)$, $P_{31}(1910)$, $P_{13}(1720)$, $D_{13}(1520)$, $P_{33}(1232)$ and $D_{33}(1700)$. The bare genuine resonances get their dressed masses and widths from the re-scattering of the baryon-meson continuum states; the $P_{11}(1440)$ (Roper) resonance appears as a dynamically generated resonance due to the strong coupling of the πN and σN channels. This hadronic model has been quite successful in reproducing the πN partial-wave amplitudes up to the center-of-mass energy of $W = 1.9$ GeV and for the total angular momentum states with $J = 1/2$ and $3/2$.

In Ref. [5] a dynamical coupled-channel model for pseudoscalar meson photoproduction based on a field-theoretical approach of Haberzettl [6] has been introduced in conjunction with the Jülich hadronic coupled-channel model. This photoproduction model is distinguished from the majority of the existing dynamical models by the fact that, in addition to satisfying unitarity and analyticity as a matter of course, it also satisfies the full gauge-invariance condition dictated by the generalized Ward-Takahashi identity. By contrast, the vast majority of existing dynamical models satisfy only current conservation but not gauge invariance. In Ref. [5], a preliminary feasibility study of this field-theory approach was presented. In the present work, we carry out an extended and more quantitative calculation of the neutral and charged pion photoproduction reactions within this approach using the Jülich πN model [3]. We calculate cross sections as well as the beam asymmetries up to $W = 1.65$ GeV.

The full single-meson photoproduction amplitude, M^μ, is obtained by attaching a photon everywhere into the dressed $NN\pi$ vertex, which gives [5]

$$M^\mu = M_s^\mu + M_u^\mu + M_t^\mu + M_{\text{int}}^\mu, \tag{1}$$
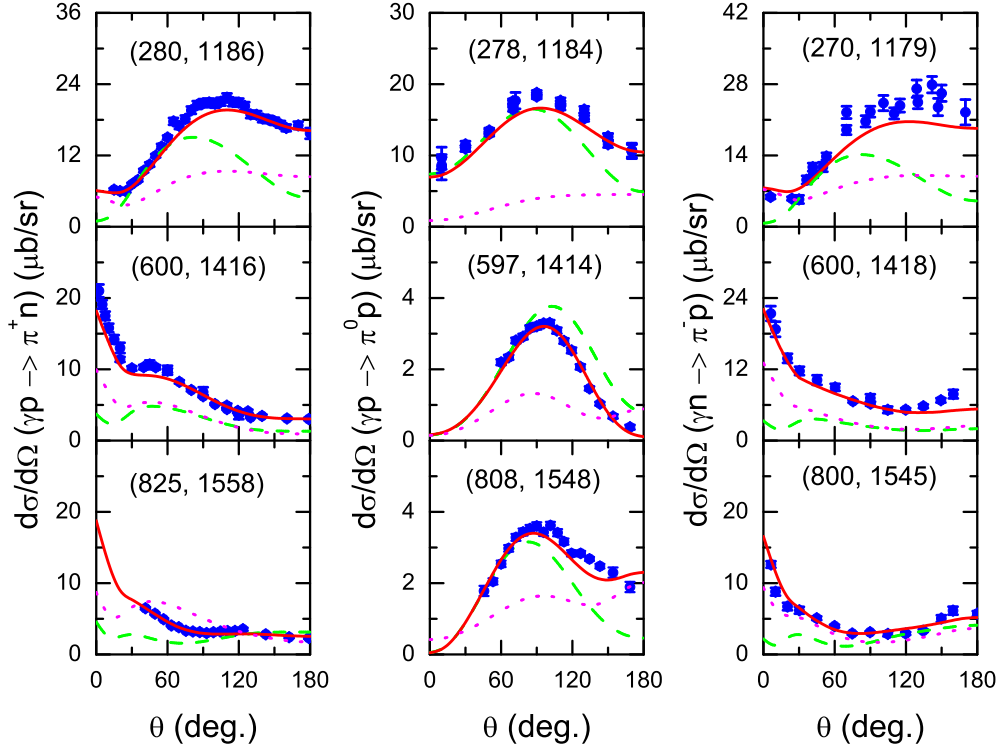
FIGURE 1. Differential cross sections for $\gamma p \to \pi^+ n$, $\gamma p \to \pi^0 p$ and $\gamma n \to \pi^- p$. The solid curves show the results from the full calculation. The dotted and the dashed curves are obtained by respectively switching off the loop integral or the contact current M_c^μ. Data are from Ref. [8].

where the first three terms describe the coupling of the photon to the external legs of the dressed $NN\pi$ vertex, with the subscripts s, u and t referring to the appropriate Mandelstam variables of their respective intermediate hadrons. The last term M_{int}^μ is interaction current, where the photon couples inside the $NN\pi$ vertex. In our work it is chosen as [5]

$$M_{\text{int}}^\mu = M_c^\mu + T^\mu + T^{NP} G_0 \left[\left(M_u^\mu + M_t^\mu \right)_T + T^\mu \right], \tag{2}$$

where $\left(M_u^\mu + M_t^\mu \right)_T$ denotes the transverse part of $\left(M_u^\mu + M_t^\mu \right)$; T^μ stands for an undetermined transverse contact current taken to be zero in the present work for simplicity; T^{NP} is the non-polar part of the hadronic scattering amplitude; G_0 describes the free propagation of the intermediate meson-baryon two-body system. M_c^μ is the generalized contact current as specified in Ref. [5]; it accounts for the complicated part of the interaction current which cannot be treated explicitly. The amplitude M_s^μ in Eq. (1) is given by

$$M_s^\mu = \Gamma_{RN\pi} S \Gamma_{RN\gamma}^\dagger, \tag{3}$$

where $\Gamma_{RN\pi}$ stands for the dressed $R \to N\pi$ vertex with R denoting either the nucleon or baryon resonance, S denotes the dressed baryon propagator. The dressed hadronic vertices and propagators are determined by the hadron dynamics of the Jülich πN coupled-channel model. $\Gamma_{RN\gamma}^\dagger$ is the full dressed $N\gamma \to R$ vertex as derived in Ref. [5].
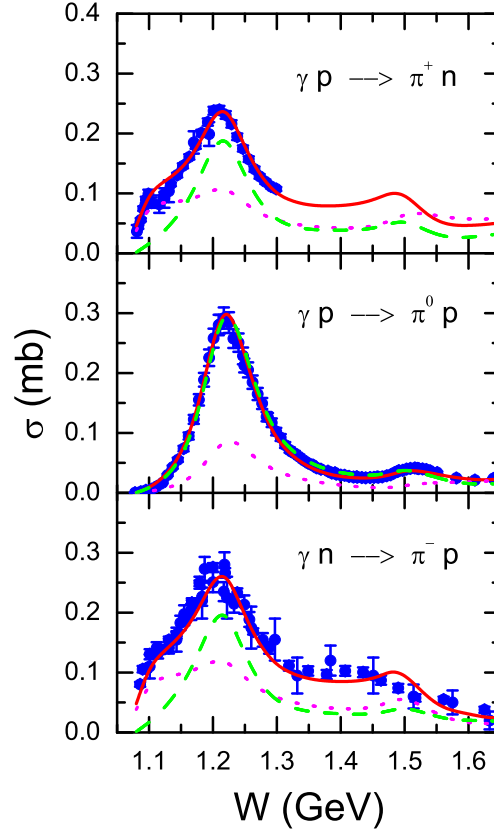
RESULTS

The parameters of the present pion photoproduction model are determined by fitting the differential cross section and the beam asymmetry data of the charged and neutral pion photoproduction up to $W = 1.65$ GeV. They are listed in
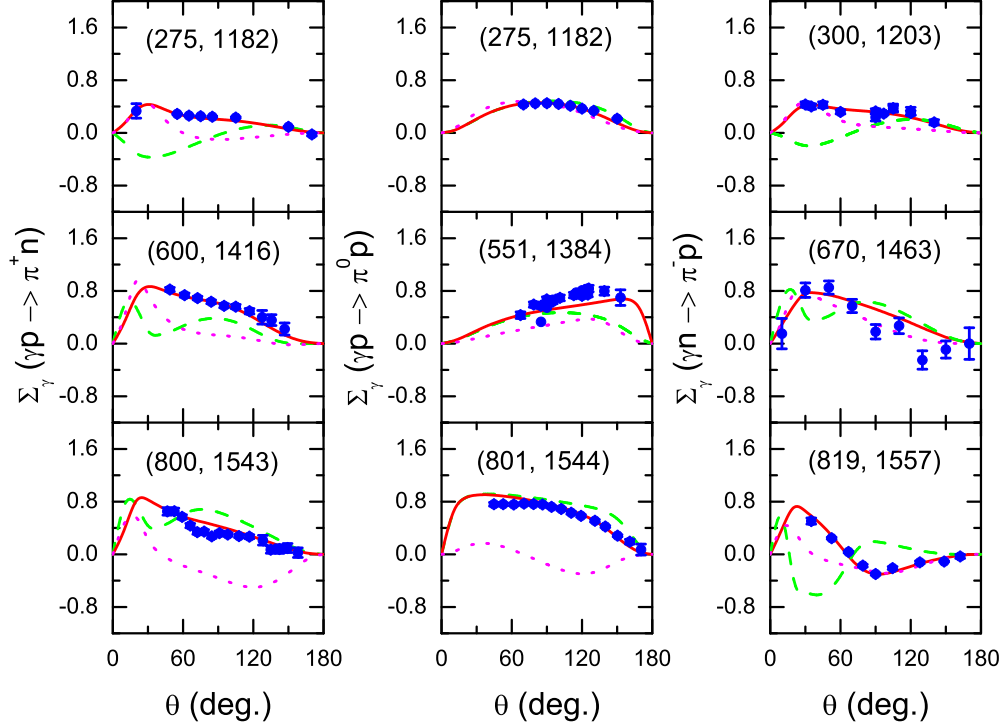
FIGURE 2. Photon spin asymmetries for $\gamma p \to \pi^+ n$, $\gamma p \to \pi^0 p$ and $\gamma n \to \pi^- p$. The solid curves show the results from the full calculation. The dotted and the dashed curves are obtained by respectively switching off the loop integral or the contact current M_c^μ. Data are from Ref. [8].

Ref. [7]. The calculated differential cross sections and beam asymmetries for $\gamma p \to \pi^+ n$, $\gamma p \to \pi^0 p$ and $\gamma n \to \pi^- p$ are shown in Figs. 1 and 2, respectively, together with the corresponding experimental data. More results for differential cross sections and beam asymmetries at 13 additional energies from the πN threshold up to $W = 1.65$ GeV can be found in Ref. [7]. Figure 3 shows the total cross sections for the three charged pion photoproduction channels. Note that the total cross-section data have not been included in our fit. In Figs. 1-3, the solid curves correspond to the results of our full calculation, while the dotted and dashed curves are obtained by respectively switching off the loop integral and the contact current M_c^μ in the full amplitude. One sees that our theoretical results for both the differential cross sections and beam asymmetries (Figs. 1 and 2) as well as the total cross sections (Fig. 3) are in good agreement with the corresponding experimental data. Juliá-Díaz *et al.* [9] have also performed an investigation of the single-pion photoproduction within the EBAC dynamical coupled-channel model. Compared to our model, they included two additional resonances, namely D_{15} and F_{15}; however, the $\gamma n \to \pi^- p$ channel was not analyzed in their work. Compared with the results of Ref. [9], the agreement of our results with the data is a little bit better for both the $\gamma p \to \pi^+ n$ and $\gamma p \to \pi^0 p$ channels. Figures 1-3 also show clearly that the loop integral and the contact current M_c^μ are important for reproducing the data, which means that the coupled-channel effects *and* gauge invariance are essential for understanding the single-pion photoproduction reactions. While the importance of coupled-channel effects was pointed out already in Ref. [9], we emphasize here that the majority of existing dynamical models of photoproduction reactions are actually not gauge invariant since their amplitudes obey current conservation only. The latter is shown in Ref. [6] to be necessary but not sufficient for maintaining full gauge invariance across all levels of a microscopic description of the photoreaction. The importance of fulfilling the gauge-invariance condition was also emphasized for the NN bremsstrahlung reaction [10].

Finally, we mention that the residues and pole positions of the full photoproduction amplitude are being evaluated in our model by making an analytic continuation of the amplitudes to complex energy plane. The results will be published

FIGURE 3. Total cross sections for $\gamma p \to \pi^+ n$, $\gamma p \to \pi^0 p$ and $\gamma n \to \pi^- p$. The solid curves show the results from the full calculation. The dotted and the dashed curves are obtained by respectively switching off the loop integral or the contact current M_c^μ. Data are taken from Ref. [8] but not included in the fit.

elsewhere.

ACKNOWLEDGMENTS

REFERENCES

1. C. Schütz, J. Haidenbauer, J. Speth, and J.W. Durso, *Phys. Rev. C* **57**, 1464 (1998).
2. O. Krehl, C. Hanhart, S. Krewald, and J. Speth, *Phys. Rev. C* **62**, 025207 (2000).
3. A.M. Gasparyan, J. Haidenbauer, C. Hanhart, and J. Speth, *Phys. Rev. C* **68**, 045207 (2003).
4. J. Wess and B. Zumino, *Phys. Rev.* **163**, 1727 (1967).
5. H. Haberzettl, K. Nakayama, and S. Krewald, *Phys. Rev. C* **74**, 045202 (2006).
6. H. Haberzettl, *Phys. Rev. C* **56**, 2041 (1997).
7. F. Huang, M. Döring, H. Haberzettl, S. Krewald, and K. Nakayama, in preparation.
8. CNS Data Analysis Center, The George Washington University, http://gwdac.phys.gwu.edu.
9. B. Juliá-Díaz, T.-S.H. Lee, A. Matsuyama, T. Sato, and L.C. Smith, *Phys. Rev. C* **77**, 045205 (2008).
10. K. Nakayama and H. Haberzettl, *Phys. Rev. C* **80**, 051001 (2009).